Unsteadiness in Effervescent Sprays – Measurement and Evaluation Using Combined PIV – PLIF Technique

Jan Jedelsky, Miroslav Jicha

Faculty of Mechanical Engineering, Brno University of Technology, Brno, Czech Republic, jedelsky@fme.vutbr.cz

Abstract Planar Laser-Induced-Fluorescence and stereoscopic Particle Image Velocimetry are simultaneously employed to study an effervescent atomizer generated spray. Light heating oil is continuously atomized using air as an atomizing medium. Double pulsed laser provides two pulses of 265 nm radiation. The pulses are converted to a light sheet illuminating the spray in a cross section perpendicular to the spray axis. Natural fluorescence of the light heating oil is used for instant liquid phase concentration distribution measurement. Simultaneous 3D velocity field is calculated using image pairs of the liquid concentration. Combination of the velocity component vertical to the laser light sheet and the concentration image leads to instant planar liquid mass flux. Set of 256 image pairs is used to calculate time averaged image of the liquid concentration and mass flux. Space-resolved fluctuations of both the values from average local value are evaluated. Root-mean-square of the liquid concentration fluctuations and mass flux fluctuations normalized by the local time-average value is used to characterise space-resolved spray unsteadiness. Results show similar spatial distribution of both the liquid concentration and mass flux. The spray is axially symmetrical with maximum of time-average mass flux (concentration) in spray axis. Radial profiles of the normalized RMS fluctuations of the mass flux (concentration) distribution show low value near the spray axis, increase with increasing radial distance and maximum close to the spray edge. Influence of atomizer operation conditions on the spray structure is also investigated. The atomizer is operated in the range of air gauge pressure 0.1 – 0.5 MPa and Gas-to-Liquid-Ratio by mass (GLR) of 2 – 50%. Results document that radial profiles of the mean values and mainly of the fluctuations of the mass flux (concentration) vary with change of operation conditions. The spray unsteadiness is relatively low in case of high GLR with increasing tendency for decreasing GLR. Influence of pressure is not so significant.

1. Introduction

Effervescent atomizers became a commonplace in industrial applications. The technology seems promising, although several operation-related issues are known; in particular spray unsteadiness observed under certain operating conditions. Its negative effects are apparent mainly in combustion process. The effervescent spray unsteadiness has been documented by several investigators (Roesler and Lefebvre 1988, Whitlow and Lefebvre 1993, Bush and Sojka 1994, Chin and Lefebvre 1995, Luong and Sojka 1999, Jedelsky and Jicha 2004, 2005a). Their results indicate that the spray unsteadiness is connected with the character of two-phase flow inside the atomizer mixing chamber. Internal two-phase flow pattern significantly depends on atomizer operation conditions (Lörcher at al. 2003, Chin and Lefebvre 1992, 1993).

Capability of spray unsteadiness quantification is necessary to detect unstable nozzle operation as well as to enable distinguishing unsteady atomizer version in the design phase or to give insight to the spray unsteadiness. So far, several methods have been developed to quantify spray unsteadiness. Method derived by Edwards and Marx (1995) uses a comparison of the measured interparticle arrival time distribution with a theoretical distribution function modelled as an inhomogeneous Poisson process. PDA system used to be employed for the interparticle arrival time measurement. This method enables to evaluate the spatial distributions of the spray unsteadiness. Possibility of classification of unsteadiness for different drop size classes is another advantage of this method. As shown in Fritsching and Heinlein (2004), Edwards (1994) and Roismann and

Tropea (2000) there are several sources of errors connected with the PDA measurements. Applications of the Edwards & Marx's method on effervescent atomizers can be found in papers of Luong and Sojka (1999), Heinlein and Fritsching (2004) and Jedelsky and Jicha (2005b).

An alternative method is based on measurement of two-phase flow pressure fluctuations in the vicinity of the exit orifice. A simplified relation between pressure fluctuations and liquid flow rate fluctuations at the exit orifice is used in Jedelsky and Jicha (2005a). The method is simple and easy to apply, it gives one value representing the overall absolute value of the spray unsteadiness at the nozzle exit for given atomizer operation conditions.

A planar droplet sizing technique, based on combined measurement of Laser Induced Fluorescence intensity and scattered light intensity of spray droplets was used by Domann and Hardalupas (2002) to quantify the spray unsteadiness of a pressure swirl atomizer. The mean and RMS of liquid volume, surface and Sauter Mean diameter (SMD) were used to evaluate the unsteadiness. Qualitative analysis of results shows existence of spray unsteadiness in the form of droplet clusters. Quantitative characterisation of liquid volume, surface area and SMD fluctuation magnitudes found that spray unsteadiness could be identified to a different extent in the three investigated RMS fields. Finally quantitative values of lengthscales and shapes of droplet clusters were taken and analyzed. Further results are given in Zimmer et al. (2003).

Presented paper describes another application of a planar imaging technique. We used a combined PIV-PLIF technique to a simple effervescent atomizer. Light heating oil was atomized, with air as the atomizing medium. Set of LIF image pairs was used to calculate instantaneous 3D velocity fields and liquid concentration in the plane perpendicular to the spray axis. Measurements were taken over a wide range of liquid flow rates and air gauge pressures. Results show spatial distribution of fluctuation of liquid mass flux and liquid concentration and assessment of the influence of operation conditions upon the spray unsteadiness. Acquired results are compared with results of some earlier investigations. The transparent atomizer used here allowed studying the mixing process and internal two-phase flow. Two-phase flow patterns predicted by published two-phase flow map and actual patterns visualized using digital camera are presented in Jedelsky and Jicha (2004, 2006).

2. Experimental facility

The experimental equipment includes an effervescent atomizer, test bench with fluid supply system and the combined PIV-PLIF system.

Atomizer description. A simplified transparent Plexiglas version of an industrial effervescent atomizer was used for the experiments. Fig. 1 is a view of the nozzle installed in the test bench. This optically accessible atomizer was mainly designed to allow an internal two-phase flow visualization (Jedelsky and Jicha, 2004). The liquid (oil) enters the central orifice on top, while the air enters by side orifices and is injected into the liquid, from each side, through a set of 15 holes with the diameter of 1 mm. The internal diameter of the mixing chamber is 8 mm and the length,

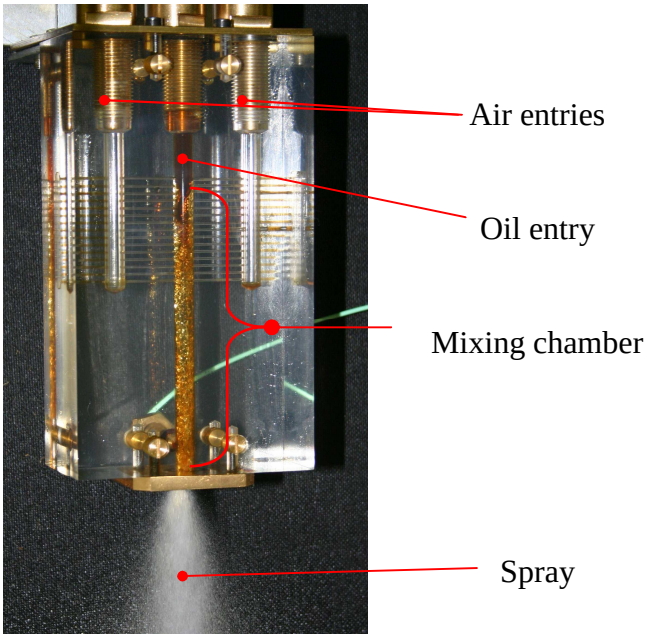

Fig. 1. Plexiglas atomizer model

downstream of the last row of air holes, is 80 mm. The two fluids form a mixture, flow downstream and exit the atomizer through an orifice to the ambient atmosphere forming a spray. The exit orifice made of brass plate has a diameter of 2.5 mm and a length of 0.7 mm. There is a conical junction with the apical angle of 90° between the orifice and the mixing tube. The atomizer described and used here is based on an early design with a long mixing chamber. It is necessary to remark that its spray is highly unsteady mainly in case of low GLR values as it will be seen later. This atomizer version is unfit for regular use, but it is suitable for new measurement method application and to observe the influence of operation conditions on the spray steadiness.

Atomizer operation. The atomizer was continuously operated and studied in the vertical downward position of the main axis. The test bench and the fluid supply system description can be found thereinafter. Physical properties of the atomized liquid – light heating oil: surface tension 0.0297 kg/s^2, density 874 kg/m^3, dynamic viscosity 0.0185 kg/(m.s). The air and oil supplies are controlled separately. Twin-fluid atomizer operation conditions can be basically described by two independent parameters. The air gauge pressure and GLR were chosen in our case. Thus other values, liquid pressure, liquid and air flow rates, are dependent upon them. Since one of the goals of this study was to investigate how the spray unsteadiness depends on the atomizer operation conditions, experiments were performed for several air gauge pressures and GLR values. Both fluids temperatures, gauge pressure and volumetric flow rates were measured.

Combined stereoscopic PIV-PLIF system. The system lay-out is seen in Fig. 2. Double pulsed Nd:YAG Continuum SLII-10 laser (1-3) equipped with 4th harmonic generator (2) provides two pulses of 265nm radiation with duration of 4ns. The laser light passing through mirrors (8) is converted by a light sheet generator (6) to a light sheet of approximately 100mm width and 2.5mm thickness, which defines the measurement plane. The light sheet illuminates the spray in a cross section perpendicular to the spray axis in the distance 152mm from the nozzle (4) exit. The image capture system consists of two TSI PIVCAM 13-8 cameras with Scheimpflug optics and 28mm lenses with appropriate optical filters (5L, 5R). The cameras are arranged in a stereoscopic setup tilted about 45° from a perpendicular view. The cameras and laser are controlled by PC (7) using synchroniser (9). Both cameras receive two images, each from one of the laser pulses. The double images are processed with a stereo PIV algorithm to provide a 3-component velocity vector field. The same images are also used for LIF intensity field, which represents the liquid density information. A series of 256 images is recorded for each experiment. Data acquisition and PIV

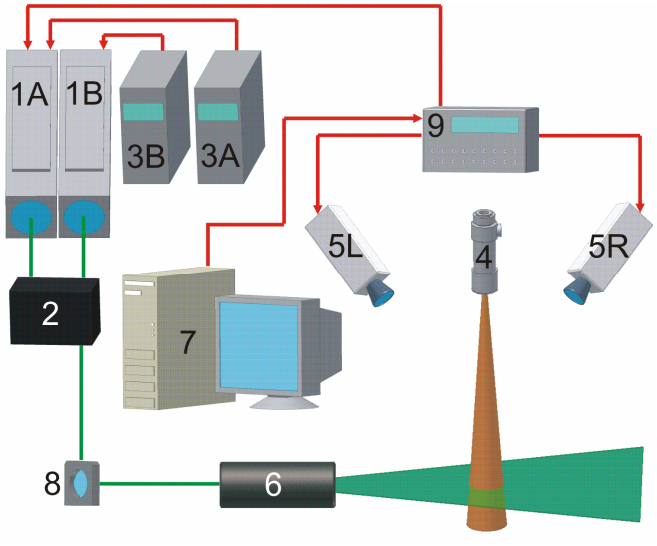

Fig. 2. Combined stereoscopic PIV-PLIF system

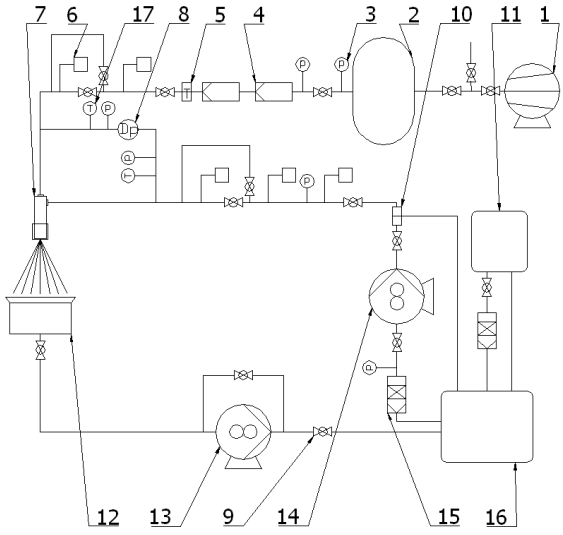

Fig. 3. Schematic layout of experimental facility

processing is made using TSI Insight 3G software. The 3-D PIV system is calibrated by a two-plane calibration target. Each single-image set is processed by PIV processor after background subtraction according this setup: Grid Engine: Deformation Grid, Spot Mask Engine: Deformation Mask, Correlation Engine: FFT Correlator, Peak Engine: Gaussian Peak, Starting spot dimension 64x64 and final spot dimension 32x32. Spurious vectors are rejected using interactive validation employing a set of Global Standard Deviation, Local Median and Local Mean filters. All additional calculations as described bellow in section Data evaluation are made using MATLAB7 software.

Test bench. A schematic layout of the experimental facility is shown in Fig. 3. It consists of a gear pump (14) that supplies light heating oil from a main fuel tank (16) through filters (15), control valves (9, 10) and flowmeters (6) into the atomizer (7). A chiller (11) ensures constant oil temperature and hence also its viscosity. The compressed air is delivered, either from the central plant, or from a two stage compressor (1), depending on the required pressure through an air chamber (2), filters (4), control valve, check valve (5) and flowmeters (6) into the atomizer. Spray is collected in a vessel (12) and returned to the main supply tank by the pump (13). The collector is connected to an oil mist separator that keeps the spray zone free of aerosol but does not disturb the spray. The gear pump (14) delivers the oil with a pressure up to 3 MPa. The fuel piping is equipped with a hydraulic shock absorber placed in front of the atomizer. Pressure (3, 8) and temperature (17) readings are taken at the atomizer inlets for both the fuel and air.

3. Data evaluation

The combined stereoscopic PIV-PLIF system is used to record a set of double images of LIF intensity field, which represents the liquid concentration $c_i(x,y)$ in the cross section (x,y) perpendicular to the spray axis. The same images are processed with a stereo PIV algorithm to provide a 3-component velocity vector field. The velocity component vertical to the laser light sheet combined with the concentration image leads to instant planar liquid mass flux:

$$\dot{m}_i(x,y) = w_i(x,y)\cdot c_i(x,y), \tag{1}$$

Instantaneous space-resolved distributions of liquid mass flux $\dot{m}_i(x,y)$ and concentration $c_i(x,y)$ are used to provide statistical information about the magnitudes of fluctuations expressing the spray unsteadiness. Recorded set of n=256 images is used to calculate the mean image representing the local mean liquid mass flux $\overline{\dot{m}}(x,y)$ and concentration $\bar{c}(x,y)$ (Fig. 5) in the cross section (x,y) perpendicular to the spray axis:

$$\overline{\dot{m}}(x,y) = \frac{1}{n}\sum_{i=1}^{n}\dot{m}_i(x,y), \tag{2}$$

$$\bar{c}(x,y) = \frac{1}{n}\sum_{i=1}^{n}c_i(x,y). \tag{3}$$

Spatial distribution of root-mean-square of liquid mass flux and concentration fluctuations normalized by the local mean value is as follows:

$$\overline{\dot{m}}'(x,y) = \frac{1}{\overline{\dot{m}}(x,y)}\sqrt{\frac{1}{n}\sum_{i=1}^{n}\left[\dot{m}_i(x,y)-\overline{\dot{m}}(x,y)\right]^2}\,, \tag{4}$$

$$\bar{c}'(x,y) = \frac{1}{\bar{c}(x,y)} \sqrt{\frac{1}{n} \sum_{i=1}^{n} [c_i(x,y) - \bar{c}(x,y)]^2} \ . \tag{5}$$

Instantaneous value of liquid flow-rate through the measurement plane can be computed from the liquid mass flux distribution:

$$\dot{M}_i = \sum_{x,y} [\dot{m}_i(x,y) \cdot s], \tag{6}$$

where s is a pixel area. RMS of flow-rate fluctuations normalized by the mean flow-rate $\overline{\dot{M}'}$ is useful for global characterisation of the spray unsteadiness. Mean value of normalized mass flux fluctuations shows an overall level of mass flux fluctuations in the measurement plane:

$$\overline{\dot{m}'} = \sum_{x,y} \overline{\dot{m}'}(x,y) \tag{7}$$

4. Results

All measurements were performed in plane perpendicular to the nozzle axis in the distance 152 mm from the nozzle exit. Influence of operation condition is investigated. Atomizer was operated with constant air gauge pressure 0.2MPa with GLR varying in range of 2-50% and with constant GLR of 5% with varying air gauge pressure in range of 0.1-0.5MPa.

Typical 3D velocity field in perspective view, averaged per 256 shots is seen on Fig. 4a. Dominant component is the axial component (the nozzle axis is identical to the Z-axis, which is perpendicular to the measurement plane). Averaged image of the Z-axis velocity component is seen on Fig. 4b. The maximum velocity agrees with the spray axis. For air gauge pressure 0.2 MPa and GLR=5% it is 35m/s. The velocity profiles correspond to results found using PDA technique in Jicha at al (2002).

Representative instantaneous concentration of liquid in the measurement plane is documented in Fig. 5a. The spray consists of small droplets in case of GLR 5% and higher. In case of very low GLR, about 2% also ligaments of the nonatomized liquid mainly near the spray axis may be observed (Fig. 5b). This phenomenon is connected with inhomogeneous two-phase mixture (plug

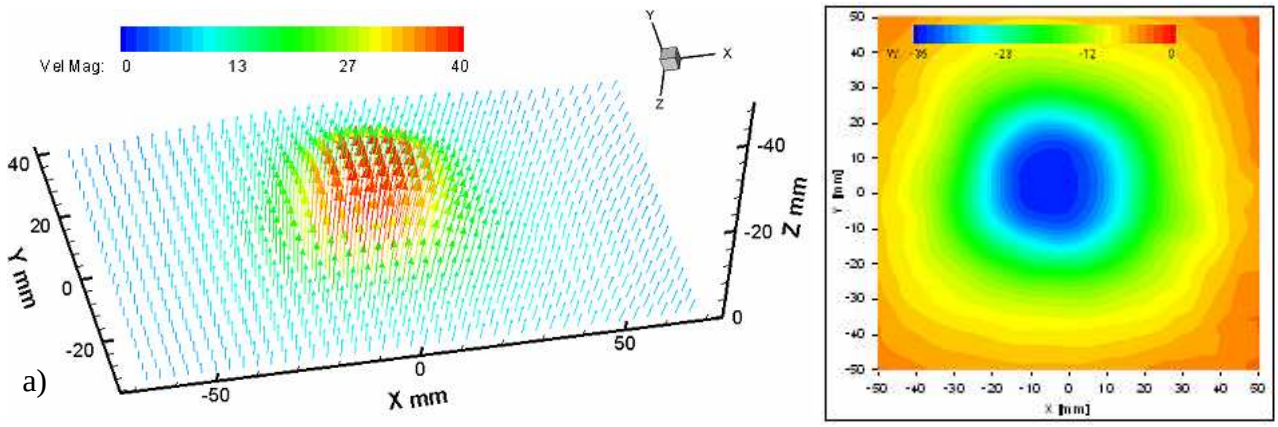

Fig. 4a. Spatial distribution of mean liquid velocity, 3D vector field in perspective view, p=0.2MPa, GLR=5%. **Fig. 4b.** Spatial distribution of mean liquid velocity, Z-component, p=0.2MPa, GLR=5%.

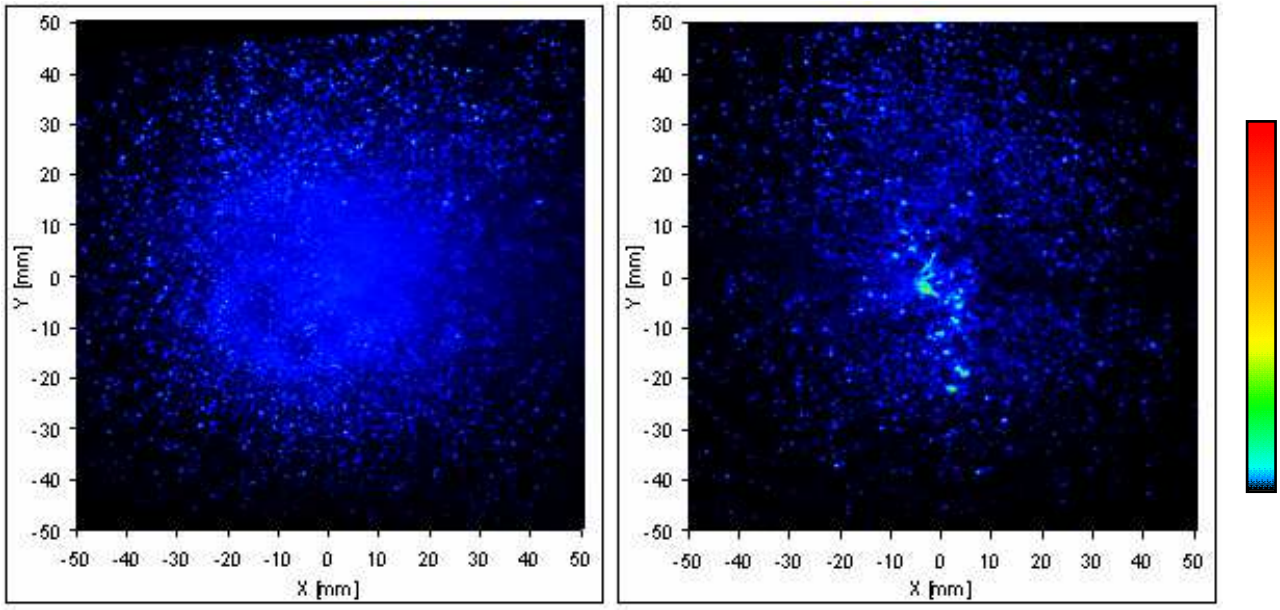

Fig. 5a. Representative spatial distribution of instant liquid mass concentration, p_a=0.2MPa, GLR=5%. **Fig. 5b.** Spatial distribution of instant liquid mass concentration with ligaments of nonatomized liquid near spray axis, p_a=0.2MPa, GLR=2%.

flow) inside atomizer and is described in Jedelsky and Jicha (2006). It is undesirable in combustion application as it can lead to increase of soot emissions and cutback of combustion efficiency.

Fig. 6 (left) documents radial distribution of the time-averaged (mean) liquid concentration for air gauge pressure 0.2MPa. Spray is axially symmetrical with maximum of the concentration in the nozzle axis. By reason of the symmetry only half profiles have been plotted. The data are normalized by their respective maximum value to enable comparison. About 90% of the liquid mass is contained in the area of 60mm in diameter in case of GLR = 2% (Fig. 6 right). Spray cone angle decreases with increasing GLR; more than 90% of liquid mass is included inside circle with 42mm in diameter for GLR = 50%. Influence of the air gauge pressure on radial distribution of the mean liquid concentration for GLR 5% is seen on Fig. 7. The influence of the pressure change on shape of the concentration profile is seen mainly near the spray axis. The liquid concentration tends to decline faster in case of low pressure. As values of the concentration near the spray axis do not affect cumulative distribution of the mean liquid concentration strongly, the cumulative distribution does not vary largely with the air gauge pressure changes. This is in contrast with the influence of GLR (Fig. 6, left), where spray is influenced more significantly in larger distance from the spray axis region and also variation of the cumulative distribution with the GLR changes is more distinct.

Radial profiles of RMS fluctuations of the liquid mass concentration normalized by the local mean liquid mass concentration are displayed in Fig. 8. The fluctuations have a low value near the spray axis and increase with the distance from the axis. The peak value lies near the spray edge. This specific pattern of the unsteadiness was also observed in PDPA measurement of spray unsteadiness by Jedelsky and Jicha (2005b). Similar results are published in papers of Luong and Sojka (1999) and Heinlein and Fritsching (2004). The spray unsteadiness shows strong influence on GLR (Fig. 8, left). The liquid mass concentration fluctuations are low in case of high GLR. The level of the fluctuations tends to increase with GLR decrease. This can be observed on the entire radial profile. In case of GLR = 2 % also growth of fluctuations near spray axis is seen. It could be caused by inferior atomization documented by areas of nonatomized liquid as mentioned above. Influence of the air gauge pressure on the fluctuations of liquid mass concentration is not as significant with the exception of the results at 0.1MPa (Fig. 8, right). Increase of the pressure mainly leads to a shift of the fluctuation maximum to higher radial distance from the spray axis.

Liquid mass flux distribution and influence of GLR on this distribution (Fig. 9) is very similar to the distribution of liquid concentration (Fig. 6). Due to weighting of concentration by axial velocity (whose maximum is situated in spray axis) the liquid mass is concentrated in a smaller region around the axis. More than 90% of liquid flows through the area of 44mm in diameter for GLR = 2%. The area decreases with GLR increase and it is 29mm for GLR = 50%. Influence of the air

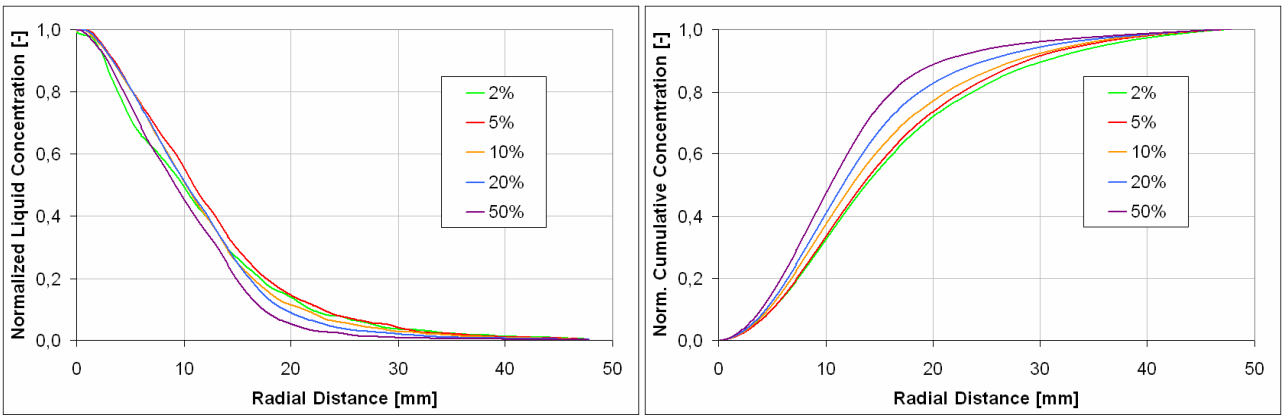

Fig. 6. Radial profiles of the normalized mean liquid mass concentration (left) and normalized cumulative mean liquid mass concentration (right) for different GLR at p_a=0.2MPa

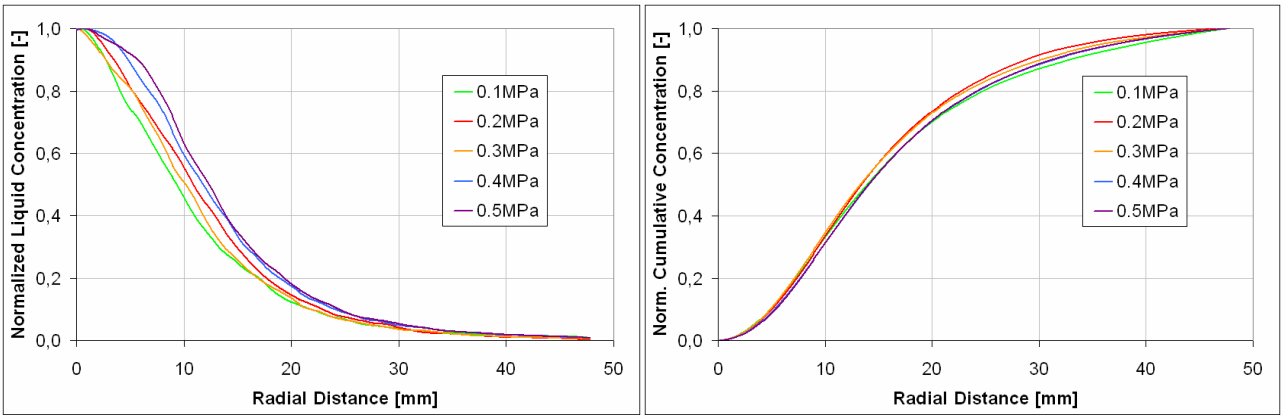

Fig. 7. Radial profiles of the normalized mean liquid mass concentration (left) and normalized cumulative mean liquid mass concentration (right) for different air gauge pressure at GLR = 5%

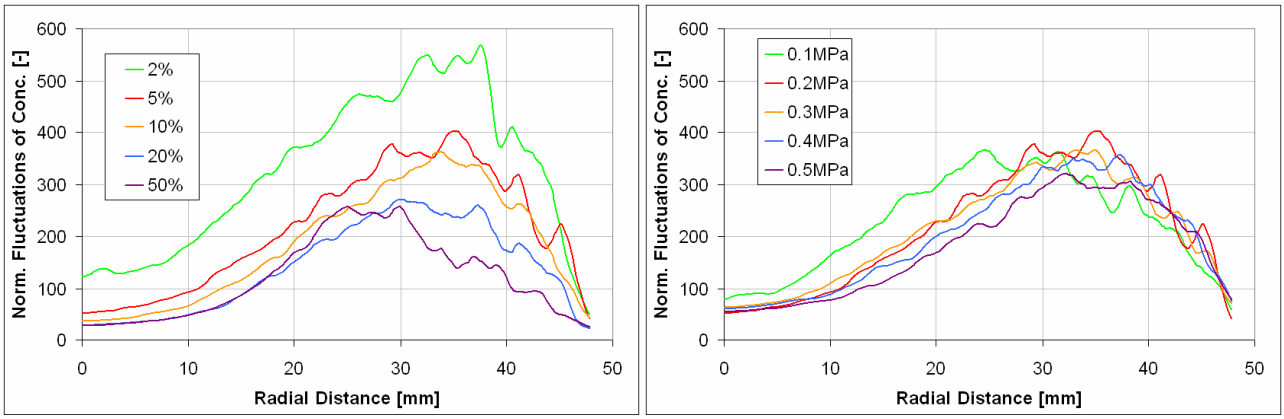

Fig. 8. Radial profiles of temporal fluctuations of the liquid mass concentration, local RMS normalized by the local mean, for different GLR at p_a=0.2MPa (left), for different air gauge pressure at GLR 5% (right)

gauge pressure on radial distribution of the mean liquid mass flux for GLR 5% is seen on Fig. 10. Increase of the pressure leads to a narrower spray cone.

Radial profiles of RMS fluctuations of the liquid mass flux normalized by local mean liquid mass concentration are documented on Fig. 11. The shape of the radial profiles as well as their variation with the air gauge pressure and GLR are comparable with the profiles of the RMS

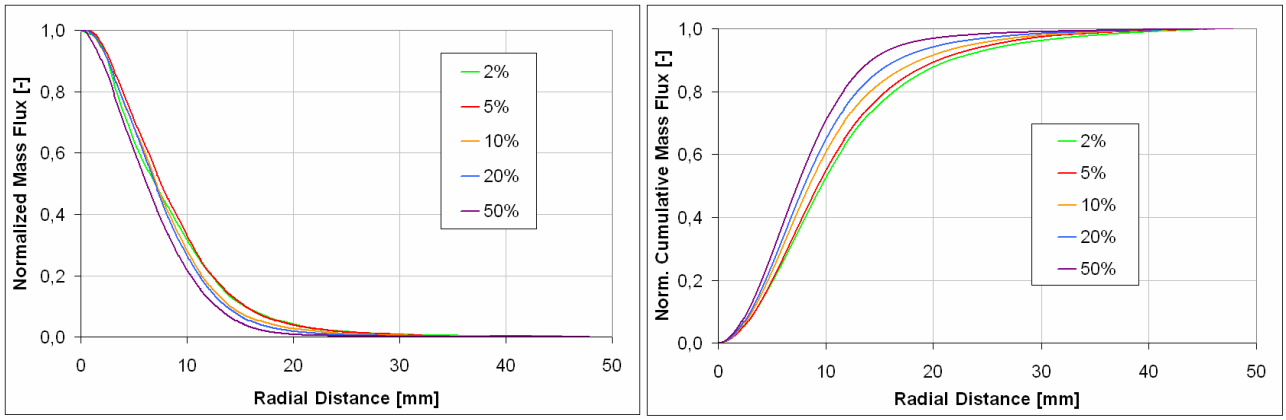

Fig. 9. Radial profiles of the normalized mean liquid mass flux (left) and normalized cumulative mean liquid mass flux (right) for different GLR at p_a=0.2MPa

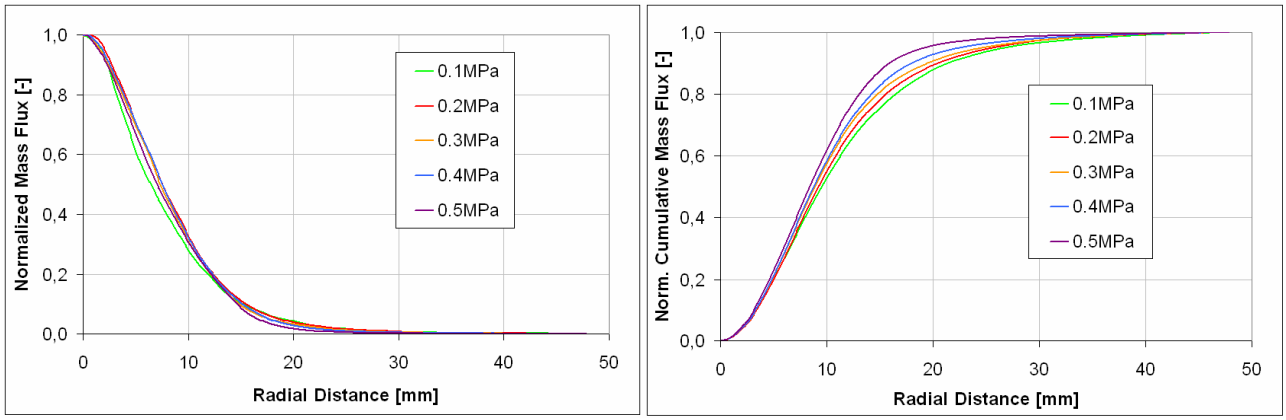

Fig. 10. Radial profiles of the normalized mean liquid mass flux (left) and normalized cumulative mean liquid mass flux (right) for different air gauge pressure at GLR = 5%

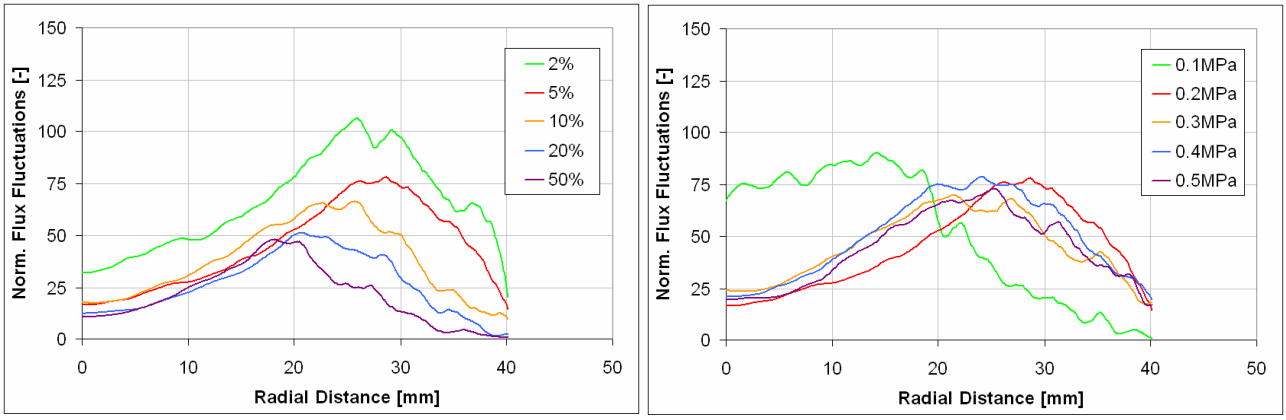

Fig. 11. Radial profiles of temporal fluctuations of the liquid mass flux, local RMS normalized by the local mean for different GLR at p_a=0.2MPa (left), for different air gauge pressure at GLR 5% (right)

fluctuations of the liquid mass concentration (Fig. 8). The maximum of the normalized liquid mass flux fluctuations is generally shifted to lower radial positions.

5. Conclusions

A method of spray unsteadiness measurement based on use of combined stereoscopic PIV-PLIF system was documented. The method was applied on simple effervescent atomizer. The space-resolved spray unsteadiness is described by means of fluctuations of liquid mass concentration and liquid mass flux normalized by their local mean values. Results show spatial distribution of the spray unsteadiness in cross section perpendicular to the nozzle axis. Both the values show similar shape of radial profiles. The effervescent spray produces generally low value of normalized mass concentration fluctuation and normalized mass flux fluctuation near the nozzle axis. The fluctuations increase with increasing radial distance and reach its maximum near the spray edge.

The effervescent spray unsteadiness depends on atomizer operation conditions. Spray is relatively stable at high GLR values while with lower GLR the unsteadiness increases. Influence of air gauge pressure is not as significant.

6. Acknowledgement

We greatly acknowledge financial support from projects GA 101/03/P020 and GA 101/06/0750 funded by the Czech grant agency.

7. Nomenclature

c	concentration	[kg/m^3]
GLR	gas-to-liquid ratio by mass	[-]
$\dot{M}$	mass flow rate	[kg/s]
$\dot{m}$	mass flux	[kg/m^2.s]
p	pressure	[Pa]
n	nuber of images	[-]
RMS	root-mean-square value	
s	pixel area	[m^2]
SMD	Sauter Mean Diameter	[μm]
w	vertical velocity component	[m/s]

subscripts

a	atomizing gas (air)
i	image consecutive number
l	atomized liquid (oil)

superscripts

$( )'$	fluctuating value
$(\bar{ })'$	root-mean-squared fluctuating value
$(\bar{ })$	time-averaged mean value

8. References

Bush SG; Sojka PE (1994) Entrainment by Effervescent Sprays at Low Mass Flowrates. Proc of the 6th ICLASS, 609-615, Rouen, France

Chin JS; Lefebvre AH (1992) Flow Regimes in Effervescent Atomization, 5th ILASS Americas, 210-214

Chin JS; Lefebvre AH (1993) Flow patterns in internal-mixing, twin-fluid Atomizers, Atomization and Sprays, Vol. 3, 463-475

Chin JS; Lefebvre AH (1995) A Design Procedure for Effervescent Atomizers, J of Eng for Gas Turbines and Power, Vol. 117, 266-271

Domann R; Hardalupas Y (2002) Planar Droplet Sizing for Quantification of Spray Unsteadiness, Proc of 18th ILASS Europe 2002, Zaragoza, Spain

Edwards CF; Marx KD; Chin WK (1994) Limitations of the ideal phase-Doppler system; Extension to spatially and temporally inhomogeneous particle flows, Atomization and Sprays, Vol. 4, 1-40

Edwards CF; Marx KD (1995) Multi-Point Statistical Structure of the Ideal Spray, Part II: Evaluating Steadiness Using the Interparticle Time Distribution, Atomization and Sprays, Vol. 5, 475-506

Fritsching U; Heinlein J (2004) Analysis of Single Point Particle Time Series for Detection of Droplet Clustering in Sprays, Proc of 3rd Int Symp on Two-Phase Flow Modelling and Experimentation, Pisa, Italy

Heinlein J; Fritsching U (2004) Droplet Clustering in Sprays, 19th ILASS Europe 2004, 412-417, Nottingham, UK

Jicha M; Jedelsky J; Otahal J; Slama J (2002) Influence of some geometrical parameters on the characteristics of effervescent atomization. Proc of 18th ILASS Europe, 345-350, Zaragoza, Spain

Jedelsky J; Jicha M (2004) Characteristics of a Two-phase Flow Inside the Mixing Chamber of an Effervescent Atomizer, Proc of 3rd Int Symp on Two-Phase Flow Modelling and Experimentation, Pisa, Italy

Jedelsky J; Jicha M (2005a) Unsteadiness of Effervescent Atomizer generated sprays. 20th ILASS Europe, 253-258, Orléans, France.

Jedelsky J; Jicha M (2005b) Unsteadiness in Effervescent Sprays – A Comparison of Two Measurement Methods and the Influence of Operation Conditions. SPRAY-05: Int Symp on Heat and Mass Transfer in Spray Systems, 55-57, Antalya, Turkey. ISBN 1-56700-223-4.

Jedelsky J; Jicha M (2006) Effervescent atomizer - temporal and spatial variations of spray structure.10th ICLASS-2006, Kyoto, Japan (In press)

Lörcher M; Schmidt F; Mewes F (2003) Flow Field and Phase Distribution Inside Effervescent Atomizers, 9th ICLASS 2003, 12-9, Sorrento, Italy

Luong JTK; Sojka PE (1999) Unsteadiness in Effervescent Sprays, Atomization and Sprays, Vol. 9, No. 1, 87-109

Roesler TC; Lefebvre AH (1988) Photographic studies on aerated-liquid atomization, combustion fundamentals and applications, Proc of the Meeting of the Central States section of the Combustion Institute, Paper 3, Indianopolis, Indiana

Roismann IV; Tropea C (2000) Drops distributions and flux measurements in sprays using phase Doppler technique, 10th Int. Symp. on Appl. of Laser Techn. to Fluid Mech., Lisbon

Whitlow JD; Lefebvre, AH (1993) Effervescent Atomizer Operation and Spray Characteristics, Atomization and Sprays, Vol.3, No.2, 137-155

Zimmer L; Domann R; Hardalupas Y; Ikeda Y (2003) Simultaneous Laser-induced Fluorescence and Mie Scattering for droplet Cluster Measurement, AIAA J, Vol. 41, No. 11